

## Annealing time effect on the properties of $CuInSe_2$ grown by electrodeposition using two electrodes system

A. Bouraiou\*

Laboratoire des Couches Minces et Interfaces, Département de Physique,  
Université Mentouri-Constantine, Constantine 25000, Algeria and  
Institut des Sciences et Technologies, Université Ziane Achour Djelfa 17000, Algeria

M.S. Aida, A. Mosbah, and N. Attaf

Laboratoire des Couches Minces et Interfaces, Département de Physique,  
Université Mentouri-Constantine, Constantine 25000, Algeria

(Received on 18 March, 2009)

In this paper, we report the effect of annealing time on the properties of copper indium diselenide  $CuInSe_2$  films. The  $CuInSe_2$  thin films have been grown at room temperature by electrochemical deposition technique using two electrodes system. The as deposited films were annealed under argon atmosphere at 300 °C during 15, 30, 45 and 60 min. The structural and morphological properties of the resulting films were characterized respectively by means of x-ray diffraction (XRD) and scanning electron microscopy (SEM). The optical band gap was estimated from transmittance measurements. We have found, that after annealing, all films present  $CuInSe_2$  in its chalcopyrite structure and with preferred orientation along  $\langle 112 \rangle$  direction. The film annealed during 45 min exhibits better crystallinity and excellent optical properties. The SEM pictures show that the elaborated films have a uniform surface morphology with a homogeneity distribution of crystallites, the grain became higher in size with prolongation of annealing time; it lays in the range of 195 to 515 Å.

Keywords: thin films,  $CuInSe_2$ , electrodeposition, annealing time

### 1. INTRODUCTION

Copper indium diselenide thin films  $CuInSe_2$  (CIS) possess direct band gap material, high optical absorption coefficient, reasonable work function, high long-term stability and largest efficiency in photovoltaic applications (it achieved an efficiency of 19 %) [1]. The homojunction and heterojunction solar cells can be prepared from this semiconductor [2]. Despite of its weak contribution to the photovoltaic market (1 %) [3], all these characteristics make the  $CuInSe_2$  one of the most promising materials for second-generation solar cells [4,5].

The efficiency of solar cells based on  $CuInSe_2$  films is critically influenced by several parameters such as the elaboration technique, the experimental parameters, the preferred orientation of  $CuInSe_2$  growth layer and substrate properties [6], etc.

$CuInSe_2$  thin films can be prepared by several methods. The electrodeposition method is probably the most appropriate and promising. This is due to its low cost, easiness, high efficiency, non vacuum and stability of the product [7,8].

In the literature there are numerous reports about the film growth by electrodeposition technique using a three electrodes system (cathode, electrode, reference electrode) [9-13]. The reference electrode has always been used to measure the cathode voltage with respect to it. On the other hand, it is an external impurity source and hence could poison the bath, and drastically reduce the efficiency of solar cells [14]. In our knowledge, Dhamardasa *et al.* [14] are the only ones who used a system with two electrodes for the deposition of  $CuInSe_2$  material.

In our work, we have grown  $CuInSe_2$  by using the elec-

trochemical deposition technique using two electrodes system, and considering its properties such as excellent electrical conduction, excellent optical transmission in the visible range (around 80 %), very significant reflectance in the infrared range, excellent adherence with the glass substrate [15], the indium tin oxide (ITO) coated glass is used as the substrate on which we deposit the films. The structural, morphological and optical properties of the resulting films were studied as a function of the annealing time.

### 2. EXPERIMENTAL

$CuInSe_2$  thin films were electrochemically deposited using two electrodes cell configurations. The instrumentation and the deposition method were the same as described in a previous work [6]. The ITO coated glass substrate is used as the working electrode (cathode). A platinum plate was used as the counter electrode (anode). A Voltammograms Multi-Potentiostat was used to control the electrodeposition process and to monitor the current and voltage profiles.

The electrolyte bath used for the films elaboration consisted of 10 mM copper chloride ( $CuCl_2$ ), 40 mM indium chloride ( $InCl_3$ ) and 20 mM selenium oxide ( $SeO_2$ ) dissolved in de-ionized water. The films were deposited at room temperature, without agitation, using a deposition potential of  $-7 V$ , and then the as deposited films were annealed under argon atmosphere at 300 °C during various heating times: 15, 30, 45 and 60 min.

The x-ray diffraction was accomplished by a Philips PZ 3710 x-ray diffractometer using monochromatic  $CuK\alpha_1$  radiation ( $\lambda=1.5406 \text{ \AA}$ ) in a scanning angle range of 10-90°. The operation voltage and current used are respectively 35 kV and 30 mA. The samples were scanned with step width of 0.02° and preset time of 2 sec. A comparison with the Joint Committee on Powder Diffraction Standards (JCPDS)

\*Electronic address: a\_bouraiou@yahoo.fr

card was done for the identification of the observed peaks. The crystallites size  $\langle D \rangle$  is calculated from the Halder and Wagner approximation [16,17].

The surface morphology of the films was observed by secondary scanning electron microscope ZEISS-SUPRA 55VP type. Spectral transmittance was recorded using Shimadzu mode UV-3101 PC spectrophotometer. The measurements were carried out in wavelengths within the range of 400-1800 nm with 2 nm steps.

The films thickness  $t$  was estimated theoretically using the following formula [18,19]:

$$t = \frac{1}{nFA} \left( \frac{isM}{\rho} \right) \quad (1)$$

Here,  $n$  is the number of electrons transferred, it was taken as 13,  $F = 96500$  C is Faraday's number,  $A$  is the electrode area,  $i$  is the applied current,  $s$  is the deposition time,  $M = 336.28$   $g\text{mol}^{-1}$  is the  $\text{CuInSe}_2$  molecular weight and  $\rho = 5.77$   $g\text{cm}^{-3}$  is the density of  $\text{CuInSe}_2$  material [20].

### 3. RESULTS AND DISCUSSION

Figure 1 (a-e) shows the x-ray diffraction patterns of the elaborated samples respectively for the as deposited film and for annealing films at  $300^\circ\text{C}$  during 15, 30, 45 and 60 min.

The peaks noted  $I$  in Fig. 1 and located at  $2\theta \approx 21.30^\circ$ ,  $30.30^\circ$ ,  $35.26^\circ$ ,  $37.42^\circ$ ,  $50.66^\circ$  and  $60.30^\circ$  correspond to the most intense peaks of ITO phase. Fig. 1(a) shows only the ITO phase, which reveals the amorphous structure of the deposited layer.

As can be seen in Fig. 1, after annealing, all the spectra appear the peaks located at  $2\theta \approx 17.10^\circ$ ,  $26.66^\circ$ ,  $27.66^\circ$ ,  $44.30^\circ$ ,  $52.50^\circ$  and  $81.38^\circ$ . These last peaks correspond to the most intense peaks given in the JCPDS card (File N°: 40-1487) for  $\text{CuInSe}_2$ , they are corresponding respectively to the (101), (112), (103), (204)/(220), (116)/(312) and (424) planes [21]. On the other hand, the calculation of the preferential orientation degree in the films [6,22] shows the high degree of preferred orientation towards the  $\langle 112 \rangle$  direction and the film annealed during 45 min presents the higher intensity ratio. This confirmed that all annealed films present a chalcopyrite phase of  $\text{CuInSe}_2$  with a tetragonal structure and with  $\langle 112 \rangle$  as preferred orientation.

The full width at half maximum FWHM and d-spacing of the (112) peak, respectively noted  $\beta_{\text{exp}}(112)$  and  $d_{112}$ , versus the annealing time are shown in Fig. 2. The inter-planar spacing  $d_{112}$  was calculated using Bragg's relation [23], the obtained values belong are in agreement with the standard JCPDS card [20].

As can be seen from the Fig. 2, the  $\beta_{\text{exp}}(112)$  follows the opposite trend of  $d_{112}$ . The  $d_{112}$  of the film annealed during 45 min is the highest one and it is closest to that given in the JCPDS card. However, the evolution of the  $\beta_{\text{exp}}(112)$  is a decreasing function of annealing time, and the (112) peak becomes narrower and more intense for the film annealed during 45 min, so this film exhibits better crystallinity. This is due to the reduction of the structure defects and internal stresses which result from the rearrangement of the atoms in the structure.

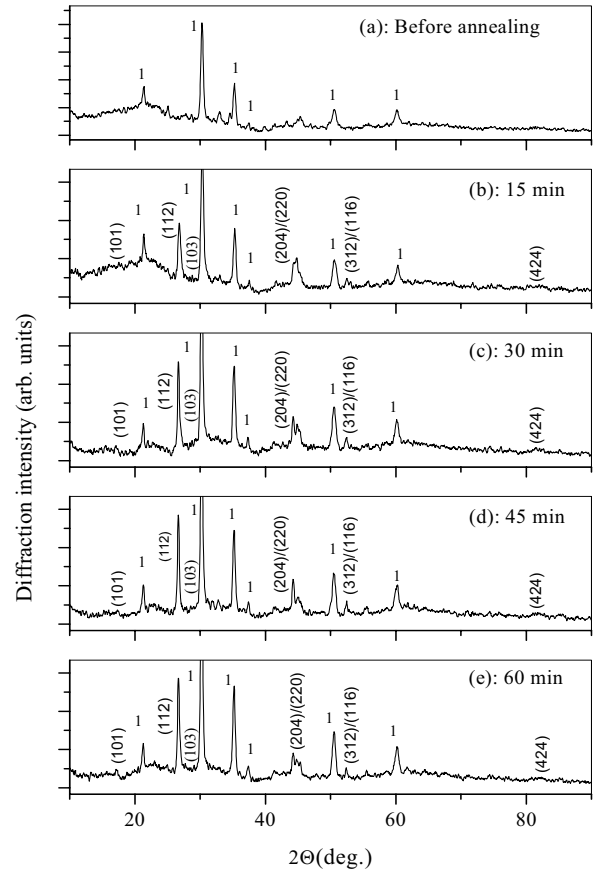


FIG. 1: XRD patterns of  $\text{CuInSe}_2$  as deposited on ITO coated glass substrate by electrodeposition technique after annealing at  $300^\circ\text{C}$  for different annealing times: (a): as deposited film, (b): 15 min, (c): 30 min, (d): 45 min and (e): 60 min. The peaks noted  $I$  correspond to the ITO phase.

In order to separate the microstrains  $\epsilon$  and crystallites size  $\langle D \rangle$  effect on the line broadening, we used the approximation introduced by Halder and Wagner [16,17]:

$$\left( \frac{\beta_{\text{stru}}^*}{d^*} \right)^2 = \frac{1}{\langle D \rangle} \frac{\beta_{\text{stru}}^*}{(d^*)^2} + \left( \frac{\epsilon}{2} \right)^2 \quad (2)$$

Where  $d^*$  is the inter-planar spacing considered in the reciprocal space and  $\beta_{\text{stru}}^*$  is given by the following relation:

$$\beta_{\text{stru}}^* = \frac{(\beta_{\text{exp}} \cos \theta)^2 - (\beta_{\text{inst}} \cos \theta)^2}{\lambda \beta_{\text{exp}} \cos \theta} \quad (3)$$

Where  $\beta_{\text{exp}}$  and  $\beta_{\text{inst}}$  are respectively the experimental and instrumental widths calculated from the diffraction spectra of the standard sample and  $\lambda$  is the radiation wavelength of the x-ray source.

After having calculated  $\beta_{\text{stru}}^*$  and  $d^*$  for the most intense peaks, we plot the  $\left( \frac{\beta_{\text{stru}}^*}{d^*} \right)^2$  evolutions versus  $\frac{\beta_{\text{stru}}^*}{(d^*)^2}$ , and we obtained a straight line. The slope reverse of this straight line represents the crystallites size  $\langle D \rangle$ . The calculated result of the crystallites size is displayed in Fig. 3. As can be seen

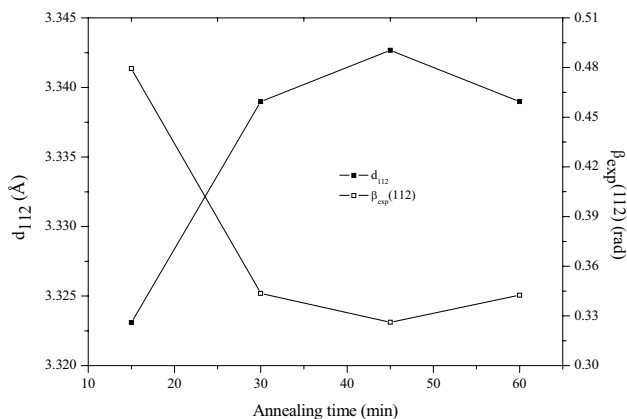


FIG. 2: β<sub>exp</sub> and d-spacing of the (112) peak as a function of annealing time.

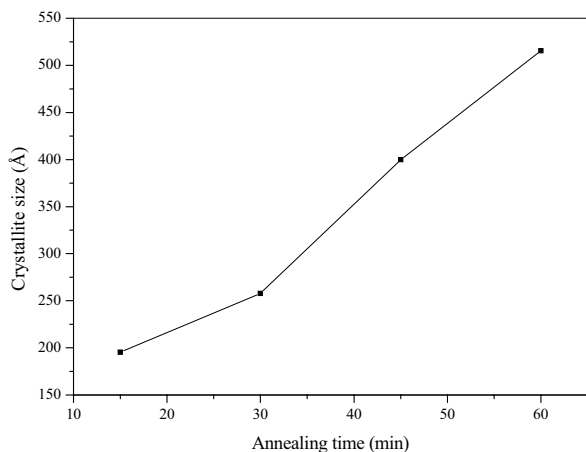


FIG. 3: Crystallite size as a function of annealing time.

from this figure, the crystallite size is a linearly increasing function of annealing time; it lays in the range of 195 to 515 Å.

The SEM micrographs of the films annealed during 15, 30, 45 and 60 min are shown respectively in Figs. 4(a-d). The film annealed during 15 min (Fig. 4(a)), shows a smooth, homogenous and small grain size. The film annealed during 30 min (Fig. 4(b)) presents a uniform surface morphology but less dense crystal structure with the appearance of a greater grain size of about 0.5 μm at the surface. The films annealed during 45 and 60 min (Figs 4(c, d)) are compact and show a good uniform surface morphology with a more dense homogeneity distribution of grains.

In order to supplement the previous analysis, we correlated the structural and morphological characterizations with optical measurements. For this, we must calculate the thickness of the as deposited films from the equation (1). We have obtained 0.9 μm.

It is well known that CuInSe<sub>2</sub> is a direct gap semiconductor, so the absorption coefficient in the region of strong ab-

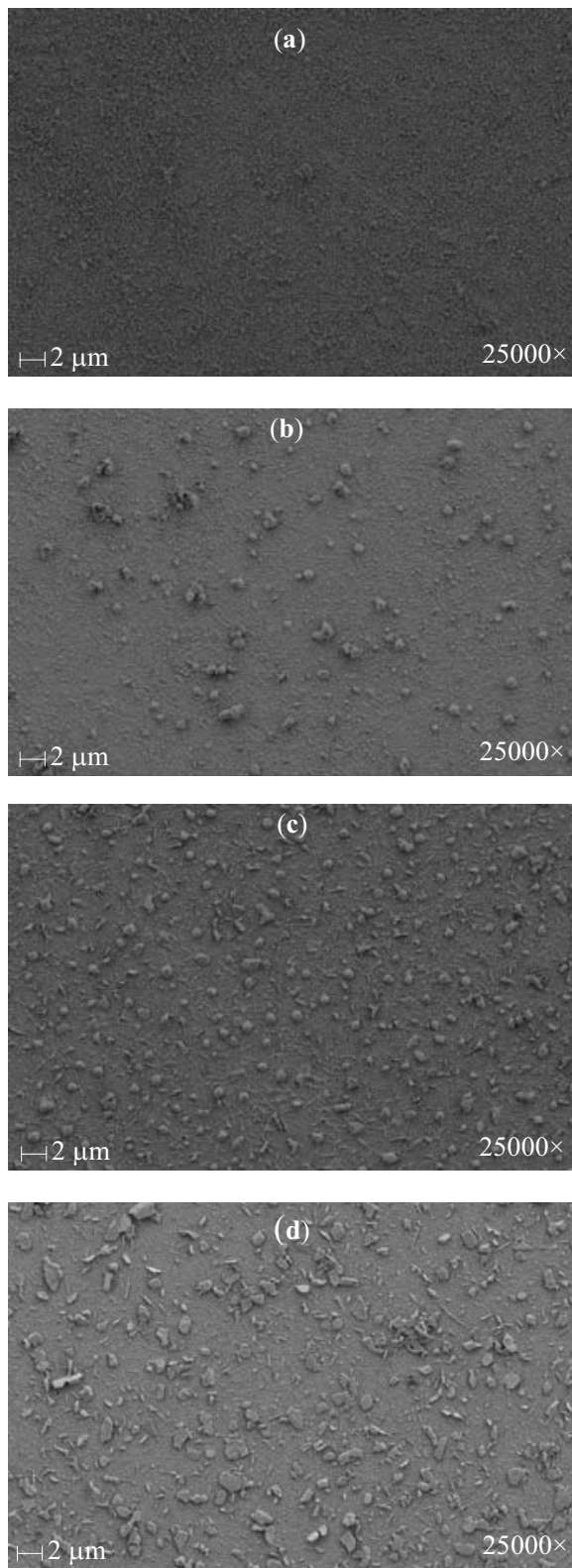


FIG. 4: SEM micrographs of elaborated thin films after annealing at 300 °C for different annealing times: (a): 15 min, (b): 30 min, (c): 45 min and (d): 60 min.

sorption obeys the following equation [24]:

$$\alpha = \frac{C}{h\nu} (h\nu - E_g)^{\frac{1}{2}} \quad (4)$$

Where  $h$  is the Planck constant,  $\nu$  is the radiation frequency,  $E_g$  is the band gap energy and  $C$  is a constant. The  $E_g$  value of the different thin films were evaluated from the plot of squares of optical absorption coefficient  $(\alpha h\nu)^2$  as function of the photon energy ( $h\nu$ ) (Fig. 5 (a-d)). The obtained results are displayed in Fig. 5.

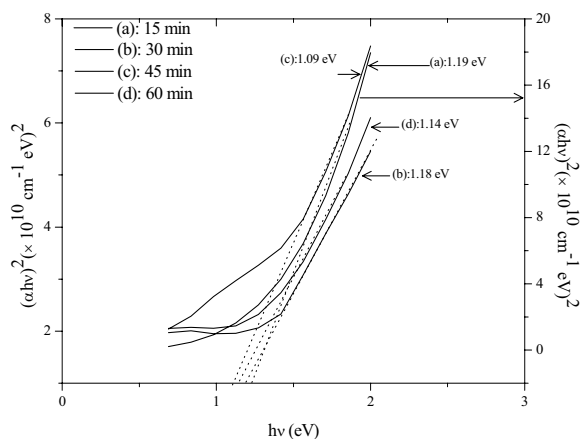


FIG. 5: Variation of  $(\alpha h\nu)^2$  as a function of radiation energy  $h\nu$  of elaborated thin films after annealing at  $300\text{ }^\circ\text{C}$  for different annealing times: (a): 15 min, (b): 30 min, (c): 45 min and (d): 60 min.

The estimated band gap was found relatively higher for

the films annealed during 15 and 30 min. However, the  $E_g$  of the film annealed during 45 min is estimated to 1.09 eV; it is lower than that of the 15, 30 and 60 min. As announced above, this decreasing can be explained by the rearrangement of the atoms in the structure and annealing of some defects with annealing time. These defects appear as deep and shallow level in the band gap of the elaborated semiconductors material. We note also that, the  $E_g$  of the last film is less than the optimum value of the terrestrial solar spectrum and it is in good agreement with the results published in the literature [25,26]. The study of the electrical properties of these films is in progress.

The films characterization suggests that the film annealed during 45 min is the optimal one for  $\text{CuInSe}_2$  production which used may be as an absorber layer in the fabrication of thin film solar cells.

#### 4. CONCLUSION

The  $\text{CuInSe}_2$  films were successfully deposited on ITO coated glass substrate using electrochemical technique. The structural, morphological and optical properties of  $\text{CuInSe}_2$  films were studied in terms of annealing time. It was found that the annealing time plays an important role in the evolution of  $\text{CuInSe}_2$  properties. Before annealing, the XRD spectra only shows the ITO phase peaks and after annealing at  $300\text{ }^\circ\text{C}$ , all the resulting films show the tetragonal chalcopyrite  $\text{CuInSe}_2$ . The average grain size of the films increases linearly with annealing time. The film annealed during 45 min exhibits better crystallinity, higher intensity ratio and a good optical properties, it can be used as an absorber layer in the fabrication of thin film solar cells.

- [1] F. Kang, J. Ao, G. Sun, Q. He, Y. Sun, J. Alloys Compd. (2009), doi:10.1016/j.jallcom.2008.12. 020.
- [2] S. Agilan, D. Mangalaraj, Sa.K. Narayandass, G. Mohan Rao, Physica B, **365** (2005) 93.
- [3] F. Abdo, Ph.D. Thesis, Institut national des sciences appliques de Lyon, France (2007).
- [4] M. Altosaar, M. Danilson, M. Kauk, J. Krustok, E. Mellikov, J. Raudoja, K. Timmo, T. Varema, Sol. Energy Mater. Sol. Cells, **87** (2005) 25.
- [5] H.T. Shaban, M. Mobarak, M.M. Nassary, Physica B, **389** (2007) 351.
- [6] A. Bouraiou, M.S. Aida, E. Tomasella, N. Attaf, J. Mater. Sci. **44** (2009) 1241.
- [7] M.E. Calixto, P.J. Sebastian, R.N. Bhattacharya, R. Noufi, Sol. Energy Mater. Sol. Cells, **59** (1999) 75.
- [8] D. Lincot, Thin Solid Films, **487** (2005) 40.
- [9] S. Moorthy Babua, A. Ennaoui, M.Ch. Lux-Steiner, J. Cryst. Growth, **275** (2005) e1241.
- [10] S.H. Kang, Y.K. Kim, D.S. Choi, Y.E. Sung, Electrochimica Acta, **51** (2006) 4433.
- [11] L. Zhang, F.D. Jiang, J.Y. Feng, Sol. Energy Mater. Sol. Cells, **80** (2003) 483.
- [12] A.A.I. Al-Bassam, Physica B, **266** (1999) 192.
- [13] J.L. Xu, X.F. Yao, J.Y. Feng, Sol. Energy Mater. Sol. Cells, **73** (2002) 203.
- [14] I.M. Dharmadasa, R.P. Burton, M. Simmonds, Sol. Energy Mater. Sol. Cells, **90** (2006) 2191.
- [15] K. Daoudi, Ph.D. Thesis, Univ. Claude Bernard - Lyon 1, France (2003).
- [16] N. C. Halder, C. N. J. Wagner, Acta Cryst. **20** (1966) 312.
- [17] R.S. Lei, M.P. Wang, M.X. Guo, Z. Li, Q.Y. Dong, Trans. Nonferrous Met. Soc. China, **17** (2007) s603.
- [18] R. Friedfeld, R.P. Raffaele, J.G. Mantovani, Sol. Energy Mater. Sol. Cells, **58** (1999) 375.
- [19] M. Faraday, Philos. Trans. R. Soc. **124** (1834) 77.
- [20] R.C. Weast (Ed.), CRC Handbook of Chemistry and Physics, CRC, Boca Raton, FL, 1980.
- [21] International Center for Diffraction Data, ICDD, PDF2 database.
- [22] J. Muller, J. Nowoczin, H. Schmitt, Thin Solid Films, **496** (2006) 364-370.
- [23] B.D. Cullity, Elements of X-Ray Diffraction, Addison-Wesley, Reading, MA, (1972) p.102.
- [24] J.C. Berned, L. Assmann, Vacuum, **59** (2000) 885.
- [25] R.P. Raffaele, H. Forsell, T. Potdevin, R. Friedfeld, J.G. Mantovani, S.G. Bailey, S.M. Hubbod, E.M. Gordon, A.F. Hepp, Sol. Energy Mater. Sol. Cells, **57** (1999) 167.
- [26] C.J. Huang, T.H. Meen, M.Y. Lai, W.R. Chen, Sol. Energy Mater. Sol. Cells, **82** (2004) 553.